Chemical characterization of organic vapors from wood, straw, cow dung, and coal burning

Tiantian Wang[1], Jun Zhang[1], Houssni Lamkaddam[1], Kun Li[1, a], Ka Yuen Cheung[1], Lisa Kattner[1], Erlend Gammelsæter[1, b], Michael Bauer[1], Zachary C.J. Decker [1, c, d], Deepika Bhattu[2], Rujin Huang[3], Rob L. Modini[1], Jay G. Slowik[1], Imad El Haddad[1], Andre S. H. Prevot[1, *], David M. Bell[1, *]

1 Laboratory of Atmospheric Chemistry, Paul Scherrer Institute, Villigen, 5232, Switzerland

2 Department of Civil and Infrastructure Engineering, Indian Institute of Technology Jodhpur, 342037, India

3 Institute of Earth Environment, Chinese Academy of Sciences, Xian 710061, China

a now at: Environmental Research Institute, Shandong University, Qingdao, 266237, China

b now at: Department of Chemistry, Norwegian University of Science and Technology, Trondheim, 7491, Norway

c now at: NOAA Chemical Sciences Laboratory (CSL), Boulder, CO 80305, USA

d now at: Cooperative Institute for Research in Environmental Sciences, University of Colorado Boulder, Boulder, CO 80309, USA

Correspondence to: Andre S. H. Prevot (andre.prevot@psi.ch) and David M. Bell (david.bell@psi.ch)

Abstract

Solid fuel (SF) combustions, including coal and biomass, are important sources of pollutants in the particle and gas phase and therefore have significant implications for air quality, climate, and human health. In this study, we systematically examined gas-phase emissions using the Vocus proton-transfer-reaction time-of-flight mass spectrometer, from a variety of solid fuels, including beech logs, spruce/pine logs, spruce/pine branches and needles, straw, cow dung, and coal. The average emission factors (EFs) for organic vapors ranged from 4.8 to 74.2 g kg^{-1}, depending on the combustion phases and solid fuel types. Despite slight differences in modified combustion efficiency (MCE) for some experiments, increasing EFs for organic vapors were observed with lower MCE. The relative contribution of different classes showed large similarities between the combustion phases in beech logs stove burning, relative to the large change in EFs observed. The $C_xH_yO_z$ family is the most abundant group of the organic vapor emitted from all SF combustion. However, among these SF combustions, a greater contribution of nitrogen-containing species and C_xH_y families (related to polycyclic aromatic hydrocarbons) is observed in the organic vapors from cow dung burning and coal burning, respectively. Intermediate volatility organic compounds (IVOCs) constituted a significant fraction of emissions in solid fuel combustion, ranging from 12.6% to 39.3%. This was particularly notable in the combustion of spruce/pine branches and needles (39.3%) and coal (31.1%). Using the Mann-Whitney U test on the studied fuels, we identified specific potential new markers for these fuels based on the Vocus measurements. The product from pyrolysis of coniferyl-type lignin and the extract of cedar pine needle were identified as markers in the spruce/pine branches and needles open burning (e.g., $C_{10}H_{14}O_2$, $C_{11}H_{14}O_2$, $C_{10}H_{10}O_2$). The product ($C_9H_{12}O$) from the pyrolysis of beech lignin was identified as the potential new marker for beech log stove burning. Many series of nitrogen-containing homologues (e.g.,

38 $C_{10}H_{11-21}NO$, $C_{12}H_{11-21}N$, $C_{11}H_{11-23}NO$ and $C_{15}H_{15-31}N$) and nitrogen-containing species (e.g.,
39 acetonitrile, acrylonitrile, propanenitrile, methylpentanenitrile) were specifically identified in cow dung
40 burning emissions. Polycyclic aromatic hydrocarbons (PAHs) with 9-12 carbons were identified with
41 significantly higher abundance from coal burning compared to emissions from other studied fuels. The
42 composition of these organic vapors reflects the burned solid fuel types and can help constrain emissions
43 of solid fuel burning in regional models.

44 **Keywords**: Vocus, solid fuel, primary emission, potential markers, combustion phase

1 Introduction

46 Solid fuels (SFs), including coal and biomass, are a primary source of domestic heating worldwide (Tao
47 et al., 2018; Oberschelp et al., 2019; Wu et al., 2022). In developing regions, such as India, more than
48 80% of rural households use biomass as cooking fuel (Balakrishnan et al., 2011). Firewood is mainly
49 used for rural households, followed by crop residues and cow dung 'cakes', which are made of a mixture
50 of dried cow dung and crop residues (Loebel Roson et al., 2021; Chandramouli and General, 2011). In
51 Europe, fireplaces and woodstoves are used for domestic heating in winter, which have considerable
52 impacts on air quality, resulting in intense 'smog' events (Kalogridis et al., 2018; Fourtziou et al., 2017;
53 Bailey et al., 2019; Font et al., 2022). China is the largest producer and consumer of coal in the world.
54 In China and some Eastern European countries like Poland, coal is widely used for domestic purposes,
55 such as heating and cooking of households, due to its cost-effectiveness and easy accessibility (Guo et
56 al., 2021; Stala-Szlugaj, 2018). The combustion of these solid fuels has been recognized as the main
57 source of anthropogenic emission of atmospheric pollutants that elicit adverse effects on air quality and
58 human health (Wu et al., 2022; Zhang and Smith, 2007).

59 Wildfires or bushfires have become more frequent in many regions due to heatwaves and drought
60 (Weber and Yadav, 2020; Williams et al., 2012). SF combustion, including wildfires, is a major source
61 of organic vapors to the atmosphere, emitting hundreds to thousands of different organic gas-phase
62 species (Hatch et al., 2019; Koss et al., 2018; Permar et al., 2021). Once emitted, evaporated vapors or
63 freshly emitted burning organic vapors will oxidize to produce oxygenated organic vapors with a broad
64 volatility range. These organic vapors with sufficiently low volatility will nucleate or condense onto
65 pre-existing aerosols to form secondary organic aerosols (SOA) (Kumar et al., 2023).

66 The identification of potential markers for each emission source will be highly valuable in evaluating
67 SOA formation potential and ambient source contributions. Liu et al. (2008) identified potential volatile
68 organic markers for different emission sources (e.g., biomass burning (BB), mobile sources and
69 painting). Nevertheless, these commonly used potential markers are well-established, yet due to their
70 presence in more than one type of biomass fuel, distinguishing between different biomass-burning
71 sources presents challenges. Since 2009, there have been many advancements in the gas-phase
72 measurements of SF, which include lab studies (Bruns et al., 2017; Bruns et al., 2016; Bhattu et al.,
73 2019) and large field campaigns (e.g., WE-CAN Aircraft Measurements, FIREX-AQ campaign)
74 (Permar et al., 2021; Jin et al., 2023; Majluf et al., 2022). However, efforts toward understanding SOA
75 formation in burning plumes have been hindered by limited identification and quantification of organic
76 vapors emitted by fires, especially intermediate volatility organic compounds (IVOCs) (Akagi et al.,
77 2011). Laboratory and field campaigns suggest that intermediate volatility organic compounds are

78 important precursors of SOA. Grieshop et al. (2009) demonstrated that traditional SOA precursors
79 account for less than 20% of the observed SOA formed from residential wood combustion emissions,
80 while IVOCs can contribute approximately 70% of the formed SOA (Li et al., 2024), which highlights
81 the urgent need for more research on IVOCs from BB emissions. Adding an IVOC emission inventory
82 to an air quality model can significantly narrow the gap between the estimated and measured SOA
83 concentrations(Li et al., 2024; Hodzic et al., 2010; Zhao et al., 2016; Robinson et al., 2007).

84 Offline sampling methods such as canisters and adsorption-thermal desorption (ATD) cartridges, along
85 with gas chromatography (GC) analysis, have limitations related to their low time resolution,
86 susceptibility to sampling artifacts, and a limited range of measurable compounds (Hatch et al., 2018;
87 Hatch et al., 2017). In addition to offline techniques, proton-transfer-reaction mass spectrometry (PTR-
88 MS) has been widely used for the online measurement of volatile organic compounds (VOCs) in the
89 atmosphere (Yuan et al., 2017). However, IVOCs still suffer from high losses in the sampling lines and
90 PTR-MS drift tubes. Furthermore, most studies have focused on either primary or aged emissions, with
91 very few examining the real-time influence of combustion conditions on the composition of emitted
92 organic vapors (Bruns et al., 2016; Akherati et al., 2020; Tkacik et al., 2017). The recently developed
93 Vocus PTR-TOF (hereafter Vocus) has greatly enhanced sensitivity due to a newly designed chemical
94 ionization source (Krechmer et al., 2018), and it can detect a broader spectrum of VOCs, IVOCs, and
95 their oxygenated products (up to six to eight oxygen atoms for monoterpene oxidation products) (Li et
96 al., 2020; Wang et al., 2021; Riva et al., 2019). With a novel design and chemical ionization source, the
97 Vocus allows for real-time characterization of gas-phase emissions during various burning phases (e.g.,
98 flaming and non-flaming phases) and identifies the potential markers for a wide range of fuels.

99 The present study compares real-time emissions from different combustion fuels. We begin by
100 demonstrating the evolution of gas-phase emissions during burning cycles highlight the changes in the
101 composition of the emissions. Then, we systematically characterize the organic vapors composition
102 using Vocus from a variety of burning fuels from both residential stoves (beech logs, spruce/pine logs,
103 and coal) and open combustion (spruce/pine branches and needles, straw, cow dung). We evaluate the
104 potential markers and EFs for different fuels and explore the dependence of individual organic vapor
105 emission intensity, variability, and chemical composition on solid fuel types and combustion phases.
106 We also discuss potential markers for the burning fuels examined in this study. The potential markers
107 are identified as statistical outliers determined with a Mann-Whitney test, consistent with previous
108 measurements (Zhang et al., 2023). The differences in EFs and profiles between different combustibles
109 can be considerable, and these results illustrate the importance of considering these emission sources
110 individually. Measurements capable of identifying and quantifying rarely measured and presently
111 unidentified emissions of organic vapors, particularly chemically complex SVOCs and IVOCs, are vital
112 for advancing the current understanding of the impact of solid fuel combustion on air quality and climate.

2 Materials and methods

2.1 Fuel and burning types

115 The experiments were conducted at the Paul Scherrer Institute (PSI) in Villigen, Switzerland. The
116 burning facility is part of the PSI Atmospheric Chemistry Simulation chambers (PACS). Real-time
117 characterization of the primary gas and particle phase emissions was carried out during 28 test burns.

118   Six solid fuels were studied (coal briquettes and biomass fuels: beech logs, spruce/pine logs, fresh
119   spruce/pine branches and needles, dry straw, cow dung) with three to six replicate burns. Material in
120   the beech, spruce, and pine fuels (e.g., logs and needles) was sourced from a local forestry company in
121   Würenlingen, Switzerland. Cow dung cakes (a mixture of cow dung and straw) were collected from
122   Goyla Dairy in Delhi, India. Coal briquettes were purchased from Gansu, China (Ni et al., 2021; Klein
123   et al., 2018).

124   With those six different fuels, we categorized six burning types for this experiment. 1) beech logs stove,
125   2) spruce/pine logs stove, 3) spruce/pine branches and needles open, 4) dry straw open, 5) cow dung
126   open and 6) coal stove. We selected these six solid fuels and conducted emissions tests to simulate
127   certain types of burning found in the atmosphere. Among the list above, 1) beech logs stove and 2)
128   spruce/pine logs stove are representative of residential wood burning, which are burned separately in a
129   stove, consistent with the materials used in two previous articles (Bertrand et al., 2017; Bhattu et al.,
130   2019). To represent forest fires or wildfire and agricultural field combustion, 3) a mixture of fresh
131   spruce/pine branches and needles and 4) straw were combusted in an open stainless-steel cylinder (65
132   cm in diameter and 35 cm in height). Traditional cooking and heating practices in regions like India are
133   represented by 5) cow dung cakes open burning by using half-open stoves (Loebel Roson et al., 2021).
134   Finally, traditional cooking and heating practices in rural regions of developing countries are
135   represented by 6) coal stove burning in a portable cast iron stove purchased from the local market (Liu
136   et al., 2017). Of course, these conditions do not fully accurately represent the conditions found in actual
137   fires, which consistent of a variety of burning species (e.g., trees, underbrush, peat soils, etc.…), but
138   represent laboratory burning conditions.

2.2 Experimental setup and instrumentation

140   The experimental design is shown in Figure S1. In summary, it is made up of a burner and a set of
141   diluters with heated lines. The zero air was provided by a zero air generator (737-250 series, AADCO
142   Instruments, Inc., USA) for cleaning and dilution (Heringa et al., 2011; Bruns et al., 2015). The zero air
143   generator takes ambient air and scrubs particulates and volatile organic compounds from the air leaving
144   a mixture that is largely made up of N_2, O_2, and Ar at ambient concentrations. Other trace gases are
145   scrubbed to lower than atmospheric concentrations including CO_2 (< 80 ppb) and CH_4 (< 40 ppb).
146   Before each burn, a continuous stream of zero air was passed through the gas lines overnight to avoid
147   cross-contamination between burns and to ensure a low background of VOCs. Once a burn is initiated
148   from the various combustibles, emissions are sampled from the chimney through a heated line (473 K).
149   The emissions (both gas and particle phases) are then diluted by two Dekati diluters (DI-1000, Dekati
150   Ltd.) which dilutes the emissions by a factor of ∼ 100 (473 K, DI-1000, Dekati Ltd.). Note that beech
151   logs combustion cycles consist of a first cycle referred to as the 'first load' and subsequent cycles,
152   referred to as 'reloads'. The first load consisted of a cold start, flaming, smoldering, and burn-out phase,
153   and the reloads were comprised of a warm start, flaming, smoldering, and burn-out phase. Organic
154   vapor emissions of solid fuel combustion are released within 10-30 min after loading according to the
155   properties of the fuels. We define the time until full ignition duration for burning encompasses 80% of
156   the entire process, starting from loading the fuels to burnout.

157   Numerous instruments were connected after the second dekati diluter for the characterization of both
158   the particulate and gaseous phases. A Scanning Mobility Particle Sizer (SMPS, CPC 3022, TSI, and

custom-built DMA) provided particle number size distribution information and calibrated by using polystyrene latex (PSL) particle size standards (Wiedensohler et al., 2018; Sarangi et al., 2017). The non-refractory particle composition was monitored by a high-resolution time-of-flight aerosol mass spectrometer (HR-ToF-AMS, Aerodyne Research Inc.). AMS data were processed using SQUIRREL (SeQUential Igor data RetRiEvaL v. 1.63; D. Sueper, University of Colorado, Boulder, CO, USA) and PIKA (Peak Integration and Key Analysis v. 1.23) to obtain mass spectra of identified ions in the *m/z* range of 12 to 120. OC (organic carbon) is derived from the ratio of organic mass (OM) to OC (OM/OC) determined with high-resolution AMS analysis (Canagaratna et al., 2015). In the AMS mass spectra, the fraction of *m/z* 60 (*f*60) represents the ratio of levoglucosan-like species (Schneider et al., 2006; Alfarra et al., 2007). AMS was calibrated for ionization efficiency (IE) by a mass-based method using NH_4NO_3 particles(Tong et al., 2021). Black carbon (BC) was measured with an Aethalometer (Magee Scientific Aethalometer model AE33) (Drinovec et al., 2015) with a time resolution of 1 minute. The maintenance and calibration are given in the AE33 user manual - version 1.57. A LI-7000 CO_2 analyzer (LI-COR) and APMA-370 CO analyzer (Horiba) provided continuous measurements of carbon dioxide (CO_2) and carbon monoxide (CO), respectively. The concentrations of total hydrocarbons (THC) and methane (CH_4) were monitored using a flame ionization detector monitor (THC monitor Horiba APHA-370).

We deployed a Vocus to measure organic vapors with a wider range of volatilities. A detailed description of the Vocus is provided elsewhere (Huang et al., 2021; Krechmer et al., 2018). For this study, the Vocus was operated with H_3O^+ as the reagent ion. The sample air was drawn in through a 1 m long polytetrafluoroethylene (PTFE) tube (6 mm o.d.) using a total sample flow of 4.3 L/min, which helped reduce the losses in the inlet wall and the sampling delay. Of the total sample flow, only 100-150 cm^3/min went to Vocus, and the rest was exhausted. The Vocus was calibrated before and after measurements every day using a multi-component standard cylinder (Tofwerk AG). Standard gases were diluted by the injection of zero air, producing mixing ratios of VOCs of around 20 ppbv. The calibration components were methanol, acetaldehyde, acetonitrile, acetone, acrylonitrile, isoprene, methyl ethyl ketone, benzene, toluene, m-xylene, α-pinene and 1,2,4-trimethylbenzene. The background measurements were performed using dry zero air every day. Data were recorded with a time resolution of 1 s. The raw data were processed using Tofware v3.2.3 software (TOFWERK, Aerodyne, Inc.). The standard non-targeted analysis workflow developed by Tofwerk was adopted for mass calibration and peak fitting. The mass transmission function and the ratios between the measured and calculated sensitivities for a series of ions were used to quantify the data and convert the ion counts to ppbv. To calculate the mixing ratio for compounds do not present in the calibration mixture, the slope of the linear fit was multiplied by the proton transfer rate constants (k_{ptr}) which have been provided in Supplement Table.

2.3 Data analysis

Modified combustion efficiency (MCE, Equation 1) is an estimate of the relative amount of flaming and smoldering and is equal to

$$MCE = \frac{\Delta CO_2}{\Delta CO + \Delta CO_2} \qquad \text{Equation (1)}$$

197 Where ΔCO, ΔCO_2 are the mixing ratios of CO or CO_2 in excess of background (measured before the
198 combustion), respectively (Christian et al., 2003). Generally, a higher MCE (> 0.9) suggests dominated
199 flaming combustion, whereas a lower MCE (< 0.9) is mostly associated with smoldering combustion
200 (Zhao et al., 2021; Zhang et al., 2022).

201 The emission factors (EFs, g kg^{-1}) of species i was calculated, following a carbon-mass balance
202 approach (Andreae, 2019; Boubel et al., 1969; Nelson, 1982):

$$EF_i = \frac{m_i}{\Delta mCO + \Delta mCO_2 + \Delta mCH_4 + \Delta mNMOGs + \Delta mOC + \Delta mBC} \times \cdot W_C \qquad \text{Equation (2)}$$

203 Here m_i refers to the mass concentration of species i. ΔmCO, ΔmCO_2, ΔmCH_4, $\Delta mNMOGs$, ΔmOC,
204 and ΔmBC are the background-corrected carbon mass concentrations of carbon-containing species in
205 the flue gas. W_C is the carbon mass fraction of the burning fuel. The W_C in the fuel a constant average
206 value of 0.46 for wood (Bertrand et al., 2017), 0.45 for straw (Li et al., 2007), 0.45 for cow dung (Font-
207 Palma, 2019), and 0.49 for coal (Zhang et al., 2000) was assumed. Changes of W_C over the burning
208 cycle are expected to be small compared to the variability of pollutant emissions. The volatility (i.e. the
209 saturation mass concentration, C^*) for individual organic compounds was calculated based on the
210 number of oxygen, carbon, and nitrogen atoms in the compound using the approach by Li et al. (2016):

$$log_{10}{}_C^* = (n_C^0 - n_C^i)b_C - n_O^i b_O - 2\frac{n_C^i n_O^i}{n_C^i + n_O^i}b_{CO} - n_N^i b_N \qquad \text{Equation (3)}$$

212 where n_C^0 is the reference carbon number; n_C^i, n_O^i and n_N^i denote the numbers of carbon, oxygen, and
213 nitrogen, respectively, in the compound. b_C, b_O and b_N are the contributions of each atom to $log_{10}{}_C^*$,
214 respectively; and b_{CO} is the carbon-oxygen nonideality. The parameters used in this analysis are
215 presented in Table S1. Most notably, the empirical approach used by Li et al. (2016) was derived with
216 only a limited number of organonitrates, which could potentially introduce bias in estimating vapor
217 pressure (Isaacman-Vanwertz and Aumont, 2021). To mitigate this bias, we modified the nitrogen
218 coefficient for CHON formulas that can be forced to equal twice the negative of the oxygen atom (b_N
219 $= -2b_O$).

2.4 Identification of potential markers

221 In this study, the relative contribution of the mixing ratio for over 1,500 species from six different fuels
222 was quantified across all 28 test burns using the Vocus. To identify the potential markers of emissions
223 from different fuels, we implemented the Mann-Whitney U test (Mann and Whitney, 1947; Wilcoxon,
224 1945) in MATLAB®. Mann-Whitney is a non-parametric test, which has been applied in the selection
225 of aerosol markers (Zhang et al., 2023), proteomic markers (White et al., 2019; Chen et al., 2012;
226 Teunissen et al., 2011; Chmaj-Wierzchowska et al., 2015; Nomura et al., 2004), and other biomarkers
227 (including measurements with a PTR-MS) (Jasperse et al., 2007; Nagai et al., 2020; Sun et al., 2019;
228 Tritten et al., 2013). It is a nonparametric test and is used for between-group comparisons when the
229 dependent variable is ordinal or continuous and not assumed to follow a normal distribution with small
230 sample sizes. This test takes two data samples as parameters, uses the ranks as a measure of central
231 tendency, and then returns the test results with a p-value to indicate the statistical significance. When
232 the p-value is lower than the significance level of 0.1 (a commonly used p-value to study statistical
233 significance in atmospheric research), the median of the tested sample is significantly high or low in

234 the two-tailed test. The molecules from a specific class of fuel that satisfy the pairwise comparison test
235 between one fuel, referred to as fuel j, and other types of fuel, were determined to be significantly high-
236 or low-fraction ions in fuel j. These ions have the potential to serve as potential markers for fuel j. We
237 have calculated in addition the fold change (FC) of ion i in fuel j was calculated using Equation 4,

$$FC_{i,j} = \frac{f_{i,j}}{f_{i,other}}$$ Equation (4)

238 Where $f_{i,j}$ represents the fraction of ion i in the mass spectra profiles of fuel j, and $f_{i,other}$ represents
239 the average fraction of ion i in the mass spectra from the other fuels. For the data used here, the

240 To identify potential markers the Mann-Whitney U test was used to compare the emissions observed
241 for one type of fuel, (e.g., spruce/pine logs) with the gaseous emissions observed for other fuels. The
242 data used for the comparison was the average composition measured throughout a full burning cycle,
243 excluding the initial ignition period. However, due to the similarity in solid fuel types between burning
244 spruce/pine logs, as well as spruce/pine branches and needles, they were categorized as separate solid
245 fuel types for this test and not compared with each other but were only compared with the other four
246 types of fuels. This could result in the loss of many same markers since these two types of fuel actually
247 come from the same type of tree. Therefore, when identifying markers for spruce/pine logs using the
248 Mann-Whitney U test, spruce/pine branches and needles were not included in the comparison group.
249 Similarly, due to the composition of cow dung 'cakes,' which are a mixture of dried cow dung and crop
250 residues, the approach used in the Mann-Whitney U test is consistent with the above method.

3 Results and discussion

3.1 The characteristics of EF and MCE from different solid fuel types

253 The average EFs of CO, CO_2, organic vapors and particular matter (PM) in g/kg as well as the MCE
254 values calculated for the 6 types of fuels, are shown in Table 1. Detailed EFs and MCE values for each
255 experiment can be found in Table S2. The average MCE value depends on the solid fuel type and the
256 combustion phase (flaming and smoldering) that is occurring. The lowest MCE values, 0.90, were
257 observed during the smoldering phase of the stove-burning of beech logs, while the highest values (0.99)
258 were recorded during the flaming phase of the spruce/pine branches and needles open burning. In all
259 experiments, the highest EFs for a single gas-phase species correspond to CO_2 (1136.2-1711.7 g/kg).
260 Coal burning has the highest average CO EFs (40.6 ± 12.6 g kg^{-1}) and CO_2 EFs (1680.2 ± 32.7g kg^{-1}).

261 Total organic vapor EFs reported in Table 1 refer to species quantified using the Vocus. The average
262 EFs of organic vapors (in the range of 4.8 to 74.2 g kg^{-1}) and the standard deviation are calculated based
263 on the average EFs for the repeatable experiments, which depend on the combustion phases and solid
264 fuel types. Generally, lower MCE values correspond to higher organic vapor EFs within a given class
265 of burning fuel (Figure S2a). For instance, smoldering beech logs resulted in significantly higher
266 average organic vapor EFs (74.2 ± 42.9 g kg^{-1}) compared to burning spruce/pine logs. Spruce/pine stove
267 and open burning, dominated by the flaming phase (average MCE > 0.95), exhibited average organic
268 vapor EFs of 44.9 ± 17.5 g kg^{-1} and 39.8 ± 11.4 g kg^{-1}, respectively. This value is higher than pervious
269 study (37.3 g kg^{-1}) even though the difference is in the uncertainty levels , which can be attributed to
270 the more extensive analysis of organic vapor in our study (Hatch et al., 2017). Despite the slight

271 difference in MCE for some experiments, the increasing EFs for organic vapors with at least six carbon
272 atoms per molecule ($\geqslant$ C6) as proxy SOA precursors were observed with lower MCE (Figure S2b)
273 (Bruns et al., 2016). Moreover, the EFs of these SOA precursors are much higher than the primary
274 biomass-burning organic aerosol (BBOA), which suggests a higher potential for SOA formation.
275 Notably, the EFs of organic vapors from cow dung and coal was relatively low, at 4.8 ± 0.98 g kg^{-1} and
276 11.5 ± 2.6 g kg^{-1}, respectively. Our EFs align well with previously reported volatile organic compound
277 EFs from bituminous coal combustion under similar conditions (range of 1.5 to 14.1 g kg^{-1}) reported by
278 Klein et al. (2018).

3.2 Comparison between flaming and smoldering of wood burning

280 Figure 1a shows a typical burning cycle during beech log wood experiments with distinct emission
281 characteristics between flaming and smoldering phases. In the top panel, the MCE, CO, and CO$_2$
282 concentrations, along with our experimental records, are used to indicate the flaming and smoldering
283 stages. The flaming phase shows considerable BC emission, while the smoldering phase is dominated
284 by organic aerosol emissions without visible flame. The absorption Ångström exponent (AAE) during
285 the smoldering phase is approximately twice that of the flaming phase, possibly due to the presence of
286 "brown carbon" in organic aerosols. f60 represents the prevalence of primary combustion products such
287 as levoglucosan and is used as an indicator for fresh BB emissions (Schneider et al., 2006; Alfarra et
288 al., 2007). During the starting/flaming phase, when the temperature is higher, f60 increases. Whereas
289 for lower temperatures in the smoldering phase, f60 decreases (Weimer et al., 2008). The mixing ratio
290 of most of the compounds correlates negatively with the MCE as expected with a significant increase
291 in the smoldering phase (Figure 1a and Figure S3). However, some compounds like benzene have
292 different enhancement rates from flaming to smoldering, which is similar to previous studies (Warneke
293 et al., 2011).

294 Figure 1b illustrates the measured EFs for flaming and smoldering wood fire stages. On average, EFs
295 for organic vapors in the flaming stage are approximately four times lower (31.4 ± 7.1 g kg^{-1}) than those
296 in the smoldering stage fires (121.9 ± 24 g kg^{-1}). Despite significant variability in the strength of organic
297 vapors emissions (EFs), the average carbon and oxygen distribution of organic vapors remained largely
298 consistent across the combustion phases (Figure S4). Hardwood (beech) is a fibrous substance primarily
299 composed of three chemical elements: carbon, hydrogen, and oxygen and these basic elements are
300 incorporated into several organic compounds, i.e. cellulose, hemicellulose, lignin, and extractives
301 formed into a cellular structure (Asif, 2009). The flaming stage is associated with more complete
302 oxidation with a relatively higher contribution of oxygenated VOCs (OVOCs, e.g., furan, oxygenated
303 aromatics, O-containing, Figure S5). Conversely, during the smoldering stage, more CO and organic
304 vapors are emitted relative to the flaming stage (Figure 1a). OVOCs, such as carbonyl, furan,
305 oxygenated aromatics, and O-containing species, form the major fraction (> 88%) of emissions in both
306 flaming and smoldering fires. They are followed by the sum of C_xH_y, and SRA (5-10%). As shown in
307 Figure S6, the volatility distribution of the emissions between the flaming phase and smoldering phase
308 changes slightly with a decrease in the IVOCs from 25.8% (flaming) to 20.2% (smoldering). Though,
309 in absolute terms all emissions are enhanced during the smoldering phase, including IVOCs, due to the
310 increased EFs during the smoldering phase. As Figure 1b shows on a relative scale that there is a higher
311 contribution of single ring aromatics and C_xH_y in the smoldering phase than flaming phase. Within these

312 measurements in our residential stove, we observe relatively small differences in the composition
313 relative to the large increase in EFs when moving from flaming to smoldering conditions.

3.3 The characteristics of organic vapor from different solid fuel types

3.3.1 Chemical composition of organic vapor from combustion

316 To assess the feasibility of distinguishing differences between combustion solid fuel types based on the
317 measured species, we evaluated the similarity of the mass spectra obtained from each experiment using
318 the correlation coefficient (r), as shown in Figure 2, organic vapors from the same burning fuel are
319 strongly correlated (0.82-0.99), indicating the general repeatability of the experiments. Furthermore,
320 we observed a weak intra-fuel correlation between coal and other biomass sources (0.44-0.78),
321 suggesting significant differences in chemical composition. By contrast, the separation between
322 different solid fuel type is not stark and all possess a correlation between 0.6-0.98. Overall, the
323 correlation coefficient highlights similarities between all biomass-based emissions, which will now be
324 discussed in detail.

325 Figure 2 also shows the average mixing ratio contribution of full ignition duration from *m/z* 40 to 300
326 for each experiment, and is categorized into C_xH_y, $C_xH_yO_z$, C_xH_yN and $C_xH_yO_zN$ families based on their
327 elemental composition. In all organic vapors, the $C_xH_yO_z$ family is the most abundant group, making
328 the largest contribution to beech logs (88.6%), spruce/pines logs (82.1%) and straw (81.7%). These
329 percentages are higher than those for coal (63.1%) and cow dung (68.9%). Coal burning results in
330 considerably higher contributions in the C_xH_y families (33.7%) than beech logs (9.3%), consistent with
331 the bulk chemical composition of the fuels.

332 Figure 3 separates emitted compounds based on their carbon (x-axis) numbers. The dominant signals
333 in organic vapors for all fuels are attributed to C3-6 compounds, while more species with higher carbon
334 numbers (#C > 10) are observed in spruce/pine branches and needles open burning. The bin containing
335 Hydrogen to carbon ratios (H/C, calculated as the ratio of hydrogen atoms to carbon atoms in a
336 molecules) between 1.2 and 1.5 has the largest contribution in all fuels except the straw, ranging from
337 27% to 31.2%. Oxygen to carbon ratios (O/C, calculated as the ratio of oxygen atoms to carbon atoms
338 in a molecule) less than 0.15 contribute significantly to coal burning (42%), which corresponds to the
339 high proportion of C_xH_y families (Figure 2). Wood and straw burning emitted more oxygenated organic
340 vapors than coal and cow dung burning with more contribution of higher O/C species (O/C> 0.5). The
341 results show similarities to the comparison between burning wood and cow dung in the particle phase
342 (Zhang et al., 2023). Specifically, cow dung exhibits a lower fraction of high O/C (0.22) compared to
343 other fuels studied.

344 We categorized organic vapors by functional groups into 10 classes based on the classifications used in
345 Bhattu et al. (2019). These classes include: alcohols, carbonyls (including acid), hydrocarbons, furans,
346 N-containing compounds, O-containing < 6 (where the number of carbon atoms is less than 6), O-
347 containing ≥ 6 (where the number of carbon atoms is equal or greater than 6), oxygenated aromatics,
348 polycyclic aromatic hydrocarbons (PAHs), single-ring aromatics (SRA). Figure S7 and Figure S8 show
349 a comparison of the organic vapor composition observed from different solid fuel types. The measured
350 emissions exhibit significantly different compositions, reflecting the variability of organic components
351 produced from different solid fuel types. The emissions of all solid fuels are overwhelmingly dominated

352 by carbonyls in the range of 23.1% (coal) to 45.1% (straw). For all emissions, furans represent the
353 second largest group, which account for more than 14% of the emissions. Comparatively, aromatic
354 compounds are less significant in BB: 5.9% - 12% for oxygenated aromatics, 0.5% - 2.1% for PAHs,
355 and 2.1% - 5.8% for SRA. In contrast, aromatic emissions are relatively larger in coal burning emissions
356 (13.6%, 8.1%, and 13.8%, respectively). Also, we note a specific difference in the oxygenated aromatic
357 compounds and those with C > 6 for open wood burning conditions, compared to the stove. This
358 difference may be driven by the difference in the water content of the wood, which is significantly
359 higher for open wood burning (30-40%) compared to stove burning (10-12%). The increase in these
360 oxygenated components comes at the expense of species containing carbonyl and furan functionalities.

361 Generally, the total fraction of nitrogen-containing species (C_xH_yN and $C_xH_yO_zN$) is significantly higher
362 in the organic vapors emitted from open burning of cow dung (18.8%) compared to the other fuels (2.1%
363 to 7.3%). This trend is consistent with both our results from aerosol composition measurement and
364 previous literature (Stewart et al., 2021b; Zhang et al., 2023; Loebel Roson et al., 2021). Generally,
365 nitrogen containing compounds in cow dung consist mainly of one nitrogen atom and have a wide range
366 of carbon numbers between 2 and 7 (Figure 3). Stewart et al. (2021a) also reported that cow dung was
367 the largest emitter of nitrogen-containing organic vapors than other fuelwood and crops in India,
368 releasing large amounts of acetonitrile and nitriles. These nitrogen-containing organic vapors are likely
369 formed from the volatilization and decomposition of nitrogen-containing compounds within the cow
370 dung cake, such as free amino acids, pyrroline, pyridine, and chlorophyll (Ren and Zhao, 2015; Burling
371 et al., 2010).

3.2.2 Volatility of organic compounds

373 The parameterization described in Sect. 2.4 uses the modified approach of Li et al. (2016) to estimate
374 the volatility of each of the measured compounds by the VOCUS in $\log_{10}(C^*)$ [µg m^{-3}]. The gaseous
375 organic compounds were grouped into a 14-bin volatility basis set (VBS) (Donahue et al., 2006) (Figure
376 4). Following the suggestions in recent papers (Wang et al., 2024; Li et al., 2023; Donahue et al., 2012;
377 Huang et al., 2021; Schervish and Donahue, 2020), the volatility was aggregated into four main classes
378 with units of µg m^{-3}: VOCs as $\log_{10}(C^*) > 6.5$, IVOCs as $\log_{10}(C^*)$ between 6.5 to 2.5, semi-VOCs
379 (SVOCs) as $\log_{10}(C^*)$ between 2.5 to - 0.5 and low-VOCs (LVOCs) as $\log_{10}(C^*) < - 0.5$).

380 Comparison and compilation of organic vapors sorted by volatility and functional group classification
381 are shown in Figure 4, and the distribution of average EFs as a function of binned saturation vapor
382 concentration is shown. The VOC class was found to be the most abundant, ranging from 58.7% to 87%
383 (Figure S9). For all burning types, carbonyls, furans, and SRA families are overwhelmingly dominant
384 in VOCs, accounting for more than 60% of the VOC emissions. The high fraction of oxygenated VOCs
385 like carbonyls in BB emissions is in stark contrast to VOCs emitted from coal combustion, which is
386 dominated by aromatic hydrocarbon emissions, particularly PAHs. This difference may be attributed to
387 the condensed structure of coal, and lack of oxygen within the fuel itself. PAHs are a group of organic
388 matter compounds containing multiple aromatic rings that mainly result from incomplete combustion
389 (Mastral and Callen, 2000).

390 IVOCs also constituted a considerable fraction in solid-fuel combustions (from 12.6% to 39.3%),
391 particularly in spruce/pine branches and needles (39.3%), cow dung (24.3%) and coal (31.1%) (Figure
392 S9). Significant differences in the bulk volatility of organic compounds were observed among different

types of wood burning. In general, spruce/pine branches and needles open burning released a higher proportion of IVOCs (39.3%) into the gas phase compared to stove logs burning (12.6% and 23.9%). This difference may be attributed to a lower percentage of terpenes in woody tissues compared to needle/leaf tissues (Greenberg et al., 2006). In addition, open burning wood has both a significantly larger water content and oxygen content than stove burning, which enhances the formation of partially oxidized organic compounds. Within the open burning experiments, the oxygenated molecules (both aromatics and C ≥ 6) are enhanced relative to the other experiments and result in the largest EF of IVOCs. In addition to the burning conditions, the fuel properties are also an important factor affecting the IVOC component. Notably, cow dung comprised a higher fraction of N-containing species within their IVOC emissions compared to other fuels. The emissions of IVOCs characterized and quantified in this study are important for the estimating and modeling of aged emissions and their propensity to be able to form secondary organic aerosol.

3.4 Chemical characteristics of dominant compounds from all biomass fuels and identification of potential markers for specific solid fuels

3.4.1 Chemical characteristics of dominant compounds from all biomass fuels

To conduct a comprehensive analysis aimed at identifying potential markers among emissions, the Mann-Whitney U test (refer to Sect. 2.5) was performed on the relative contribution of primary organic vapors derived from various fuels as measured by the Vocus. The results of the pairwise Mann-Whitney test are presented in Figure S10, illustrating the average $-log_{10}$ p-value as a function of the log_2 fold change (FC). Species that yield p-values lower than 0.1 in the two-tailed test for all pairwise comparisons are deemed significantly more abundant or scarce in a particular solid fuel type compared to all other fuels. These species are indicated as colored circles in Figure 5. In cases where species do not meet this criterion once or multiple times, they are represented as gray circles, even if their average p-value falls below 0.1. A higher $-log_{10}$ (p-value) signifies a reduced likelihood that the fractional medians of two species are equivalent. Simultaneously, a greater FC (as per Equation 4) indicates an increased presence of the species' fractional contribution in the tested fuel in comparison to the average contribution across all other fuels. This suggests a higher degree of exclusivity for this species in the given context. The potential markers, p-values, fold changes, and threshold results are listed in the Supplement Table.

As shown in Figure 2, biomass fuels (such as logs, branches, needles, straw, and cow dung) were analyzed separately from coal due to their distinct characteristics. To address this distinction, we characterized the dominant compounds across various biomass fuels by setting a threshold (relative mixing ratio contribution ≥ 0.1%) for compounds that are not potential markers of one specific biomass fuels. This approach allowed us to identify compounds that are more readily detectable in complex environments. As shown in Figure S11, the gas-phase analysis revealed several dominant compounds: $C_5H_4O_2$ (furfural, 2.2-10.1%), $C_2H_4O_2$ (acetic acid, 2.1-5.8%), $C_3H_6O_2$ (methyl acetate, 1.7-4.6%), and C_2H_4O (acetaldehyde, 1.3-3.9%), which were also reported prior studies on BB (Bruns et al., 2017; Stockwell et al., 2015; Christian, 2004; Sarkar et al., 2016). Furthermore, the category of dominant compounds represents the primary set of compounds associated with BB, contributing from 46% to 69% of the emissions (Figure S12). Carter et al. (2022) expand the representation of fire organic vapors in a global chemical transport model, GEOS-Chem, which contributes substantially to atmospheric

434   reactivity, both locally and globally. Our results could provide more input information for global or
435   regional chemistry transport models.

3.4.2 Identification of potential markers for specific solid fuels

437   Mass defect plots of potential markers are visualized in Figure 5, for each burning source, respectively.
438   Many potential markers are identified for each unique type of burning (Supplement Table). As shown
439   in Figure 5, potential markers of all wood burning are mainly composed of compounds from the C_xH_y
440   and $C_xH_yO_z$-family. However, the potential markers for spruce/pine branches and needles have higher
441   molecular weights and are more oxidized, which aligns with their characteristics of the mass spectrum.
442   In contrast, compounds from open burning of straw and cow dung contribute considerably more to
443   nitrogen-containing families but less to oxygen-containing species, consistent with their bulk chemical
444   composition characteristics. Additionally, potential markers for coal consist mainly of compounds from
445   C_xH_y-family, which also aligns with its bulk chemical composition and relatively higher H/C ratios
446   (Figure 3).

447   For all softwood (i.e., spruce/pine logs and spruce/pine branches and needles in this study),
448   monoterpenes ($C_{10}H_{16}$) are a potential marker along with the fragment at m/z 81.07 (C_6H_8). However,
449   monoterpenes cannot exclusively be related to BB given their abundance in the atmosphere.
450   Monoterpenes are also the biogenic volatile organic compounds (BVOCs) emitted from natural trees
451   and other vegetation (Hellén et al., 2012). However, the emission rates of terpenes vary with season,
452   with a higher rate in spring and summer and a lower rate in autumn and winter (He et al., 2000; Noe et
453   al., 2012). In winter, monoterpenes could be a potential marker for softwood burning due to minor
454   natural emissions from spruce, but in summer, terpene emissions from natural trees would dominate the
455   contribution making it a non-potential marker. P-cumenol ($C_9H_{12}O$), as one of the potential markers for
456   beech logs, was discovered to be one of the prominent products of beech wood pyrolysis of lignins
457   (Sengpiel et al., 2019; Keller et al., 2020). Homologues of $C_{10}H_{8-18}O_2$ are determined for spruce/pine
458   branches and needles, with $C_{10}H_{10}O_2$ being β-phenylacrylic acid, which is one of the main chemical
459   compositions of the extract of the cedar pine needle. $C_{10}H_{14}O_2$ could be 1-guaiacylpropane, which is
460   proposed as a potential marker for coniferyl-type lignin pyrolysis products from pine (Simoneit et al.,
461   1993; Liu et al., 2021). Homologues of $C_{11}H_{8-18}O_2$ are also seen, for example, $C_{11}H_{14}O_2$, likely 1-(3,4-
462   dimethoxy-phenyl)-1-propene, which is stated as a representative compound found in lignin (Alves et
463   al., 2003; Hill Bembenic, 2011).

464   Noticeably, cow dung has a significantly different chemical composition. As a result, many potential
465   markers are identified from the burning of cow dung compared to other fuels. These potential markers
466   predominantly contain nitrogen in chemical composition and overlap all potential markers for straw,
467   owing to the mixture of dried cow dung and crop residues in "cow dung cakes." Many nitrogen-
468   containing potential markers are found in straw and cow dung, such as C_4H_5N, C_5H_5N, C_5H_7N, and
469   C_6H_7N, which could likely be assigned to pyrrole, pyridine, methylpyrrole and methyl pyridines
470   respectively. Pyrolysis of the constituents in the crop residue is a probable pathway for these compounds
471   (Ma and Hays, 2008). Acetonitrile (C_2H_3N), acrylonitrile (C_3H_3N), propanenitrile (C_3H_5NO), and 4-
472   methylpentanenitrile ($C_6H_{11}N$) were found as potential markers for cow dung with generally higher FC
473   and higher relative contribution. Additionally, several series of nitrogen-containing homologues are
474   found, such as $C_{10}H_{11-21}NO$, $C_{12}H_{11-21}N$, $C_{11}H_{11-23}NO$ and $C_{15}H_{15-31}N$. These nitrogen-containing gases

have also been detected, especially in emissions from cow dung cake in India compared to fuelwood and are likely formed from the volatilization and decomposition of nitrogen-containing compounds within the cow dung cake. These compounds originate primarily from free amino acids but can also arise from pyrroline, pyridine, and chlorophyll (Stewart et al., 2021a).

Coal is also a distinct solid fuel compared to other biomass fuels in this study, showing a relatively lower correlation coefficient (Figure 2). Consequently, many series of C_xH_y-family homologues are found. Compounds with 9-12 carbon atoms, as shown in Figure 5 for coal burning, could be PAHs-related, such as C_9H_8 (1-Indene), $C_{10}H_8$ (naphthalene), $C_{10}H_{10}$ (1-methylnapthalene), $C_{12}H_{10}$ (acenaphthene), $C_{12}H_{12}$ (2,6-dimethylnaphthalene). The EFs of the potential markers also show an increasing trend with the decrease of MCE (Figure S13), which suggests EFs of the potential markers are not only dependent upon the type of fuel burnt but also on the burning condition.

4 Conclusions

In this study, we investigated emissions of organic vapors using Vocus during typical solid fuel combustion, including burning of beech logs, spruce/pine logs, spruce/pine branches and needles, straw, and cow dung and coal briquettes. Average EFs of CO, CO_2, organic vapors and PM were calculated. This work provides a comprehensive laboratory-based analysis of the chemical composition of organic vapors emitted from the different combustibles and different combustion phases. We discuss the prominent net combustion emissions from BB and identify new potential markers using the Mann-Whitney U test.

The results indicate that wood burning has higher organic vapors EFs compared to other fuels. The emissions varied significantly, ranging from 4.8 to 74.2 g kg^{-1}, depending on the combustion phases and solid fuel types. Despite the slight difference in modified combustion efficiency (MCE) for some experiments, the increasing EFs for organic vapors were observed with lower MCE. Moreover, the EFs of these SOA precursors are much higher than the primary biomass-burning organic aerosol (BBOA), which suggests a higher potential for SOA formation. Distinct particulate/gas emissions at different combustion phases are observed for stove burning of beech logs: initial compositions of flaming or smoldering plumes were dominated by BC or OA, respectively, with much higher organic vapor emission in smoldering. The relative contribution of different classes showed large similarities between the combustion phases in beech logs stove burning, relative to the large change in EFs observed. Therefore, the enhanced EFs under smoldering conditions means there is a greater potential for SOA formation when compared to flaming conditions.

The $C_xH_yO_z$-family is the most abundant group (63.1% to 88.6%) for all solid fuels, followed by C_xH_y (9.3% to 33.7%). A larger contribution of nitrogen-containing species (C_xH_yN and $C_xH_yO_zN$) is found in cow dung burning, while coal burning has a higher contribution from the C_xH_y families. Moreover, the VOC class was found to be the most abundant (58.7% to 87%), followed by the IVOC class (12.6% to 39.3%). Primary semivolatile/intermediate-volatility organic compounds (S/IVOCs) have been proposed as important SOA precursors from BB. Li et al. (2024) found that IVOCs from residential wood burning (~ 13% of total organic vapors) can contribute ~70% of the formed SOA. Overall, these data will help update the IVOC emission inventory and improve the estimates of SOA production. Specifically, these results demonstrate that open burning (e.g., wildfire) emissions have enhanced IVOC

EFs, suggesting that the SOA potential from open-burning sources is larger in comparison to their wood stove counterparts.

However, each source generally emits a wide spectrum of organic vapors species, leading to considerable overlap between organic vapors species from different sources. Based on the Mann-Whitney U, we selected species that were unique in certain emissions as possible potential markers for specific solid fuels and the dominant compounds for all biomass fuels. Due to minor natural emissions from spruce in summer, monoterpene ($C_{10}H_{16}$) and its fragment could be potential markers for all softwoods (i.e., pine logs and spruce/pine branches and needles in this study) in winter. More products of the pyrolysis of coniferyl-type lignin and the cedar pine needle extract could be found in spruce/pine branches and needles open burning (e.g., $C_{10}H_{14}O_2$, $C_{11}H_{14}O_2$, $C_{10}H_{10}O_2$). The prominent product ($C_9H_{12}O$) resulting from the pyrolysis of beech lignin is identified as the potential markers for beech log stove burning. Many series of nitrogen-containing homologues and nitrogen-containing species (e.g., acetonitrile, acrylonitrile, propanenitrile, methylpentanenitrile) are identified (e.g., $C_{10}H_{11-21}NO$, $C_{12}H_{11-21}N$, $C_{11}H_{11-23}NO$ and $C_{15}H_{15-31}N$), particularly from open burning of cow dung. Coal is a unique solid fuel compared to biomass and more PAHs-related potential markers are identified from coal burning with 9-12 carbon. These potential markers provide important support for future global or regional chemistry transport modeling and source apportionment. Overall, our study provides a comprehensive understanding of the molecular composition and volatility of primary organic compounds, as well as new insights into the identification of potential markers from the burning of solid fuels.

Tables and figures

Table 1 Average EFs of CO, CO_2, organic vapors and PM as well as MCE for 6 types of Solid fuel type.

Solid fuel type	Carbon content	MCE	Emission factors (g kg^{-1} fuel)			
			CO	CO_2	organic vapors	PM
beech logs stove (n=6)	0.46	0.96 ± 0.03	38.9 ± 25.9	1409.4 ± 177.1	74.2 ± 42.9	2.5 ± 1.7
spruce/pine logs stove (n=5)	0.46	0.97 ± 0.01	28.5 ± 14.3	1511.7 ± 68.5	44.9 ± 17.5	1 ± 0.6
spruce/pine branches and needles open (n=3)	0.46	0.99 ± 0.001	2.8 ± 0.8	1579.2 ± 29.7	39.8 ± 11.4	0.9 ± 0.4
straw open (n=4)	0.45	0.97 ± 0.01	24.4 ± 6.6	1488.4 ± 87.2	42.6 ± 33.7	2.8 ± 0.7
cow dung open (n=5)	0.45	0.95 ± 0.03	53.9± 27.2	1541.8 ± 50.2	4.8 ± 0.98	1.2 ± 0.61
coal stove (n=5)	0.49	0.96 ± 0.01	40.6 ± 12.6	1680.2 ± 32.7	11.5 ± 2.6	0.9 ± 0.3
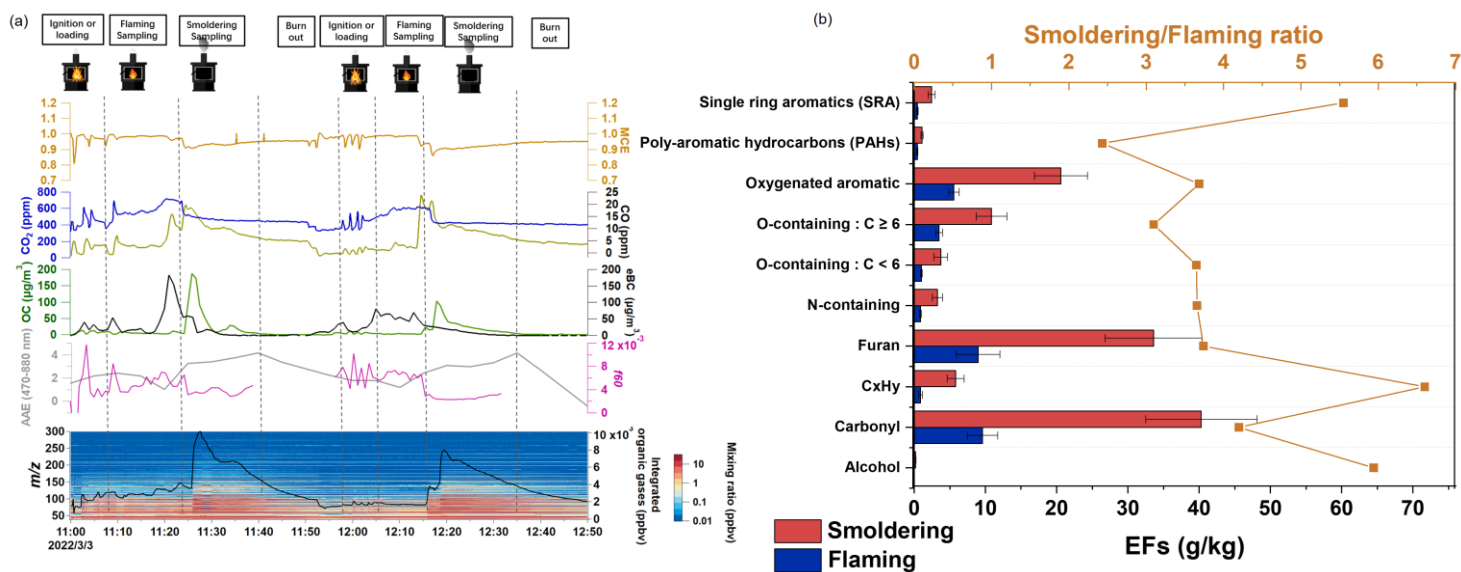
Figure 1. (a) Temporal profiles of mixing ratios measured by Vocus and evolution of CO, CO_2, AAE, $f60$, MCE and key aerosol compositions during burning cycles of beech logs stove burning (b) Geometric mean of the primary EFs for gas-phase species of different functional groups during flaming and smoldering phase, respectively (the flaming and smoldering was separated by the experimental record and calculated MCE). Error bars correspond to the sample geometric standard deviation of the replicates. The square represents the mixing ratio between smoldering and flaming. In this study, the MCE is used to indicate the flaming stage and smoldering and a significant decrease of MAC and CO_2 was observed from the flaming phase to the smoldering phase.

560
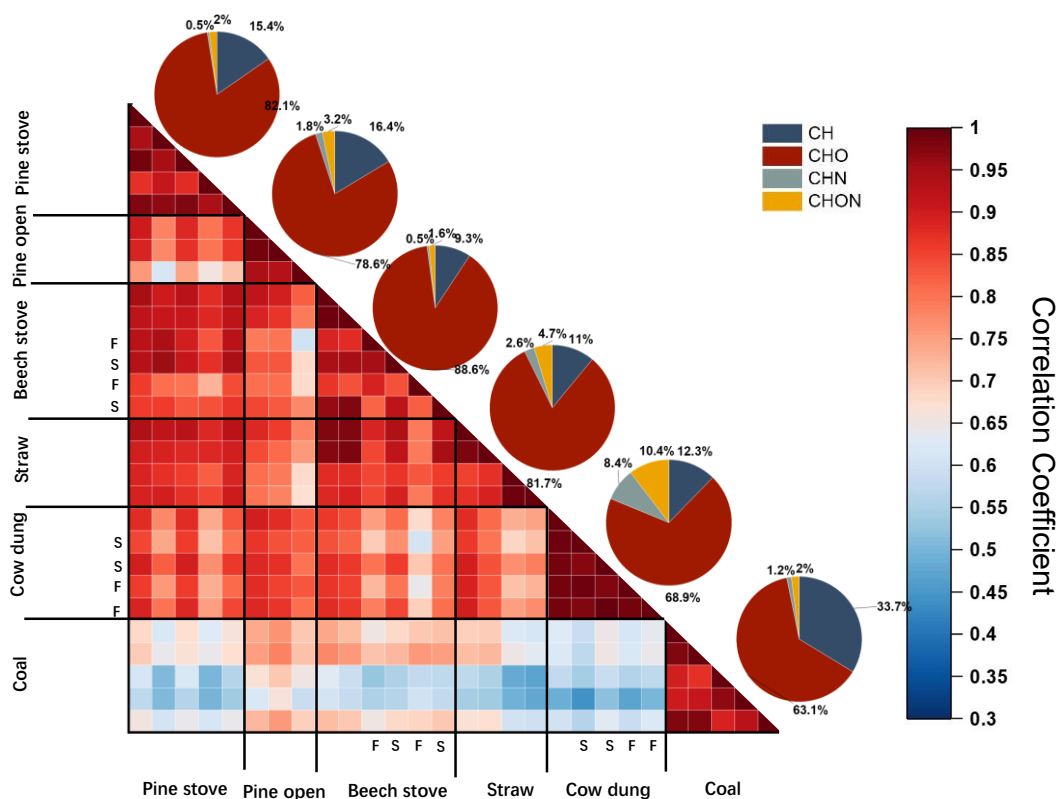
Figure 2. The correlation matrix of organic vapors measured with Vocus (F represents flaming phase and S represents smoldering phase and unmarked columns and rows represent mixtures of both flaming and smoldering phases). Pie charts showing the contribution of elemental families are on the diagonal.

564
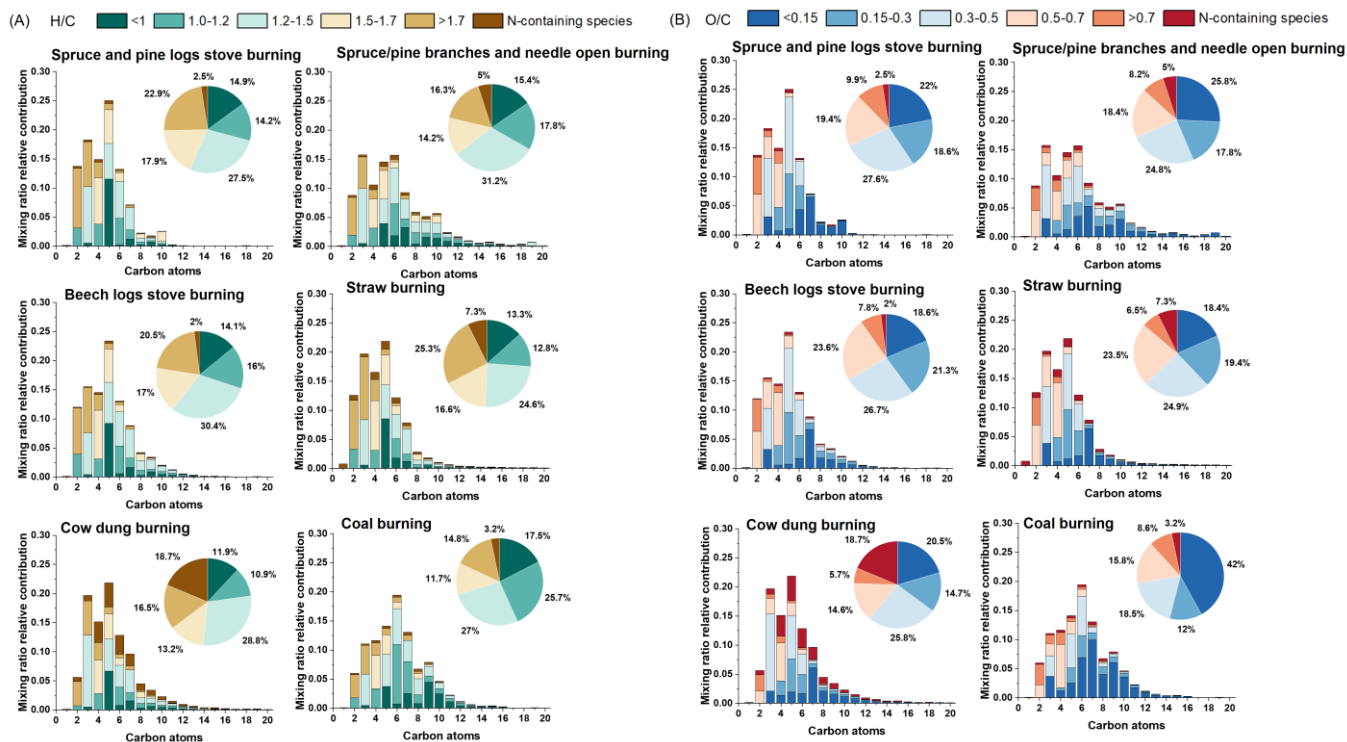
Figure 3. The average carbon distribution is colored by the H/C (**A**) and O/C (**B**) for non-N-containing species. The pie charts are the corresponding contribution of a range of H/C or O/C ratios.

567
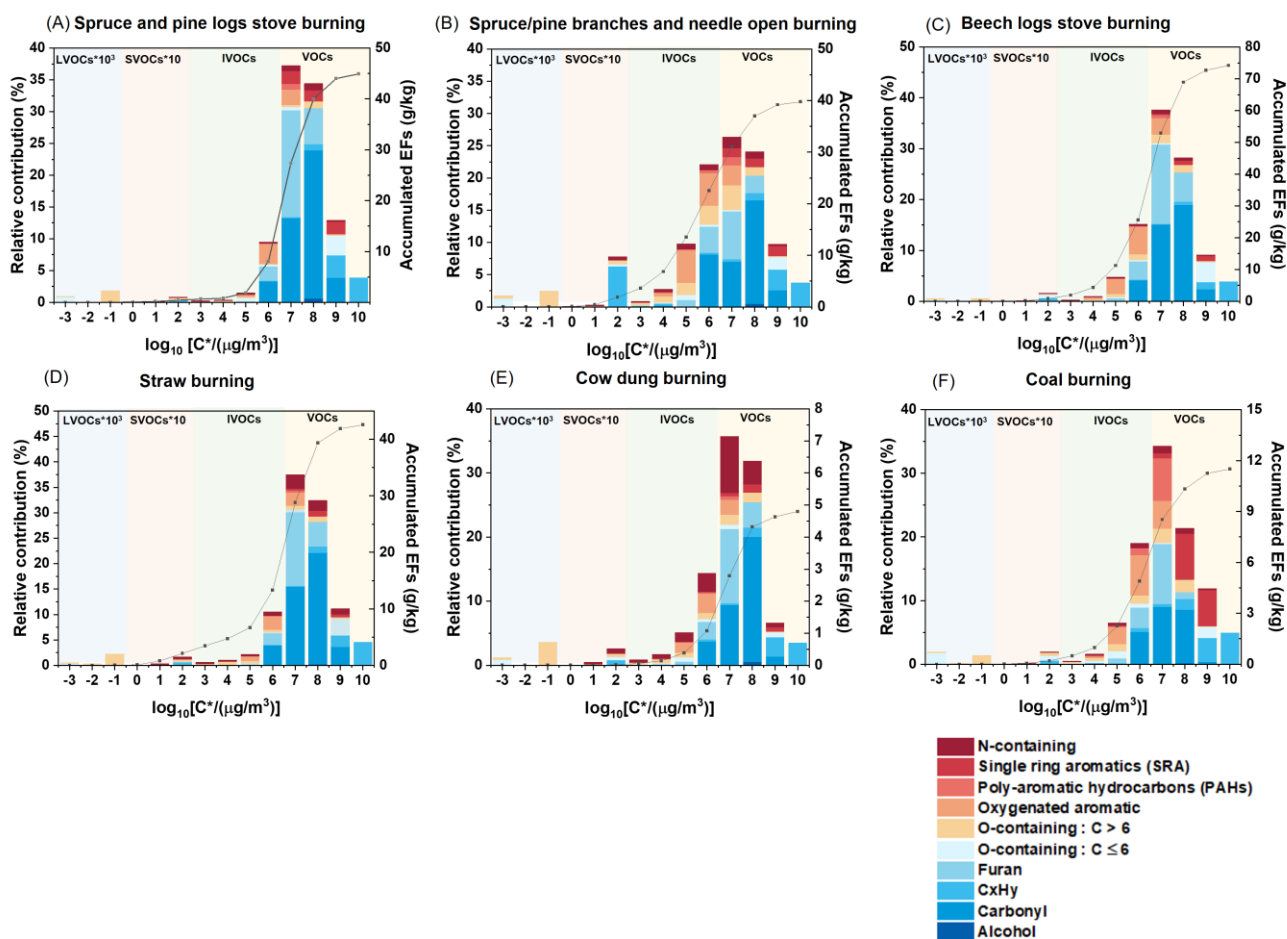
568 **Figure 4.** Volatility and average accumulated EFs (assume the average molecular weight of each bin are same)
569 the distribution of primary emissions as a function of binned saturation vapor concentration. Shaded areas indicate
570 the volatility ranges with units of μg m^{-3}: VOCs (yellow) as $\log_{10}(C^*) > 6.5$, IVOCs (blue) as $\log_{10}(C^*)$ between
571 6.5 to 2.5, semi-VOCs (SVOCs, green) as $\log_{10}(C^*)$ between 2.5 to - 0.5 and low-VOCs (LVOCs, orange) as
572 $\log_{10}(C^*) < - 0.5$. The relative contribution of LVOCs and SVOCs are multiplied by a factor of 1000 and 10,
573 respectively.

574
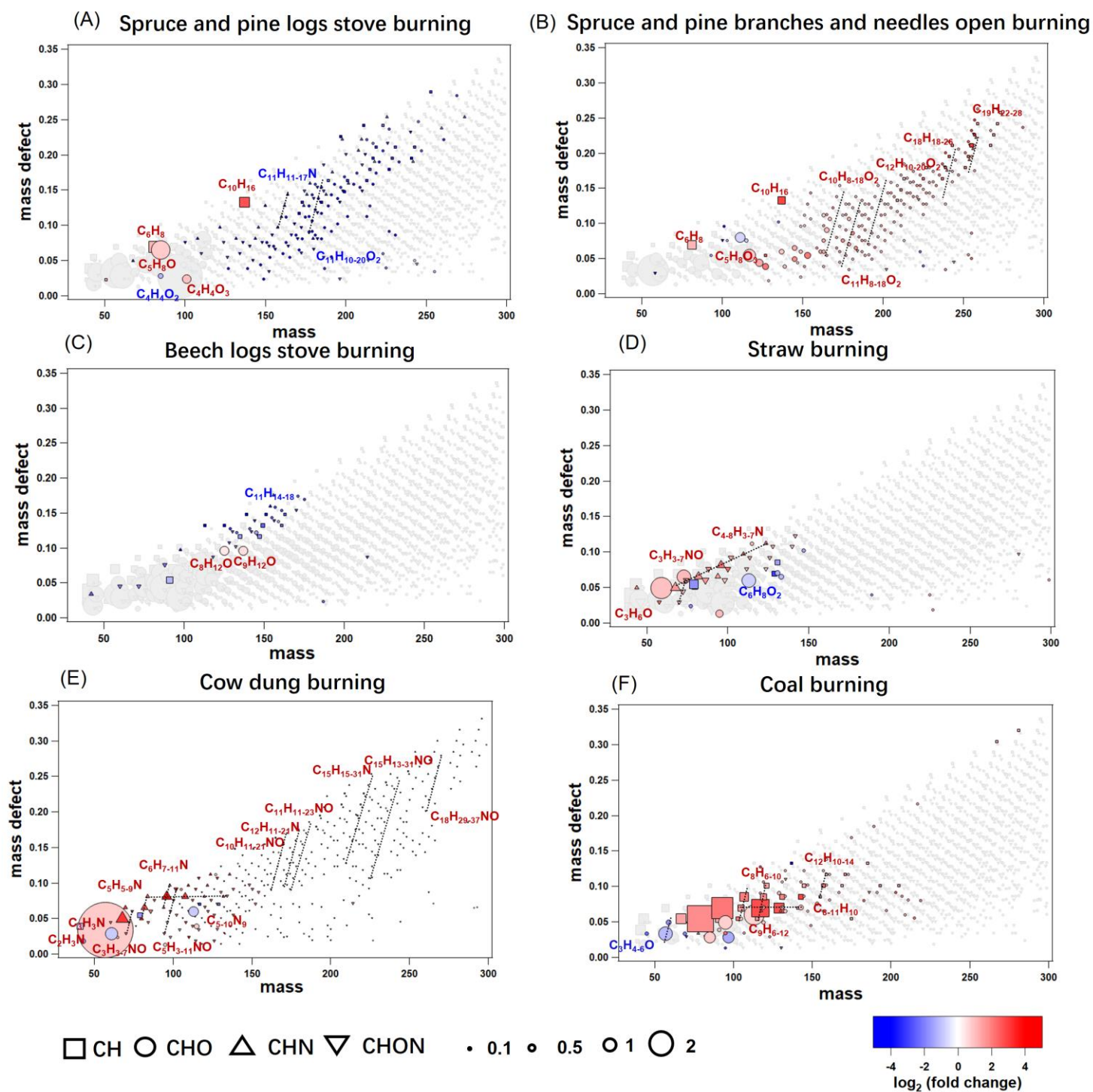
Figure 5. Mass defect plots identifying potential markers sized by the square root of fractional contribution (%) and colored by log$_2$ (the fold change). The dashed line represents the series of homologues.

Data availability

The data presented in the text and figures are available in the Zenodo online repository (https://doi.org/ 10.5281/zenodo.14204572).

Author contributions

TTW, JZ, HL, KL, RKYC, EG, LK, DMB, and RLM conducted the burning experiments. TTW analyzed the data and wrote the paper. MB, ZCJD, LK, DMB, KL, RLM, IEH, HL, JGS, and ASHP participated in the interpretation of data.

Competing interests

The authors declare that they have no conflict of interest.

Acknowledgments

This work was supported by the Swiss National Science Foundation (SNSF) SNF grant MOLORG (200020_188624), an SNSF Joint Research Project (grant no. IZLCZ0_189883), the PSI career return fellowship, and the European Union's Horizon 2020 research, innovation programme under the Marie Skłodowska-Curie grant agreement No 884104 (PSI-FELLOW-III-3i) and ATMO-ACCESS. PSI's atmospheric simulation chamber is a facility of the ACTRIS ERIC and receives funding from the Swiss State Secretariat for Education, Research and Innovation (SERI grant).

Reference

Akagi, S., Yokelson, R. J., Wiedinmyer, C., Alvarado, M., Reid, J., Karl, T., Crounse, J., and Wennberg, P.: Emission factors for open and domestic biomass burning for use in atmospheric models, Atmos. Chem. Phys., 11, 4039-4072, 2011.

Akherati, A., He, Y., Coggon, M. M., Koss, A. R., Hodshire, A. L., Sekimoto, K., Warneke, C., de Gouw, J., Yee, L., Seinfeld, J. H., Onasch, T. B., Herndon, S. C., Knighton, W. B., Cappa, C. D., Kleeman, M. J., Lim, C. Y., Kroll, J. H., Pierce, J. R., and Jathar, S. H.: Oxygenated Aromatic Compounds are Important Precursors of Secondary Organic Aerosol in Biomass-Burning Emissions, Environ. Sci. Technol., 54, 8568-8579, 10.1021/acs.est.0c01345, 2020.

Alfarra, M. R., Prevot, A. S., Szidat, S., Sandradewi, J., Weimer, S., Lanz, V. A., Schreiber, D., Mohr, M., and Baltensperger, U.: Identification of the mass spectral signature of organic aerosols from wood burning emissions, Environmental science & technology, 41, 5770-5777, 2007.

Alves, V., Capanema, E., Chen, C.-L., and Gratzl, J.: Comparative studies on oxidation of lignin model compounds with hydrogen peroxide using Mn (IV)-Me3TACN and Mn (IV)-Me4DTNE as catalyst, J. Mol. Catal. A: Chem., 206, 37-51, 2003.

Andreae, M. O.: Emission of trace gases and aerosols from biomass burning–an updated assessment, Atmos. Chem. Phys., 19, 8523-8546, 2019.

Asif, M.: Sustainability of timber, wood and bamboo in construction, in: Sustainability of construction materials, Elsevier, 31-54, 2009.

Bailey, J., Gerasopoulos, E., Rojas-Rueda, D., and Benmarhnia, T.: Potential health and equity co-benefits related to the mitigation policies reducing air pollution from residential wood burning in Athens, Greece, Journal of Environmental Science and Health, Part A, 54, 1144-1151, 2019.

618   Balakrishnan, K., Ramaswamy, P., Sambandam, S., Thangavel, G., Ghosh, S., Johnson, P., Mukhopadhyay, K.,
619   Venugopal, V., and Thanasekaraan, V.: Air pollution from household solid fuel combustion in India: an
620   overview of exposure and health related information to inform health research priorities, Global health action,
621   4, 5638, 2011.
622   Bertrand, A., Stefenelli, G., Bruns, E. A., Pieber, S. M., Temime-Roussel, B., Slowik, J. G., Prévôt, A. S. H.,
623   Wortham, H., El Haddad, I., and Marchand, N.: Primary emissions and secondary aerosol production
624   potential from woodstoves for residential heating: Influence of the stove technology and combustion
625   efficiency, Atmos. Environ., 169, 65-79, 10.1016/j.atmosenv.2017.09.005, 2017.
626   Bhattu, D., Zotter, P., Zhou, J., Stefenelli, G., Klein, F., Bertrand, A., Temime-Roussel, B., Marchand, N., Slowik,
627   J. G., Baltensperger, U., Prevot, A. S. H., Nussbaumer, T., El Haddad, I., and Dommen, J.: Effect of Stove
628   Technology and Combustion Conditions on Gas and Particulate Emissions from Residential Biomass
629   Combustion, Environ. Sci. Technol., 53, 2209-2219, 10.1021/acs.est.8b05020, 2019.
630   Boubel, R. W., Darley, E. F., and Schuck, E. A.: Emissions from burning grass stubble and straw, Journal of the
631   Air Pollution Control Association, 19, 497-500, 1969.
632   Bruns, E. A., El Haddad, I., Slowik, J. G., Kilic, D., Klein, F., Baltensperger, U., and Prevot, A. S.: Identification
633   of significant precursor gases of secondary organic aerosols from residential wood combustion, Sci Rep, 6,
634   27881, 10.1038/srep27881, 2016.
635   Bruns, E. A., Slowik, J. G., El Haddad, I., Kilic, D., Klein, F., Dommen, J., Temime-Roussel, B., Marchand, N.,
636   Baltensperger, U., and Prévôt, A. S. H.: Characterization of gas-phase organics using proton transfer reaction
637   time-of-flight mass spectrometry: fresh and aged residential wood combustion emissions, Atmos. Chem.
638   Phys., 17, 705-720, 10.5194/acp-17-705-2017, 2017.
639   Bruns, E. A., El Haddad, I., Keller, A., Klein, F., Kumar, N. K., Pieber, S. M., Corbin, J. C., Slowik, J. G., Brune,
640   W. H., Baltensperger, U., and Prévôt, A. S. H.: Inter-comparison of laboratory smog chamber and flow
641   reactor systems on organic aerosol yield and composition, Atmos. Meas. Tech., 8, 2315-2332, 10.5194/amt-
642   8-2315-2015, 2015.
643   Burling, I., Yokelson, R. J., Griffith, D. W., Johnson, T. J., Veres, P., Roberts, J., Warneke, C., Urbanski, S.,
644   Reardon, J., and Weise, D.: Laboratory measurements of trace gas emissions from biomass burning of fuel
645   types from the southeastern and southwestern United States, Atmos. Chem. Phys., 10, 11115-11130, 2010.
646   Canagaratna, M. R., Jimenez, J. L., Kroll, J. H., Chen, Q., Kessler, S. H., Massoli, P., Hildebrandt Ruiz, L., Fortner,
647   E., Williams, L. R., Wilson, K. R., Surratt, J. D., Donahue, N. M., Jayne, J. T., and Worsnop, D. R.: Elemental
648   ratio measurements of organic compounds using aerosol mass spectrometry: characterization, improved
649   calibration, and implications, Atmos. Chem. Phys., 15, 253-272, 10.5194/acp-15-253-2015, 2015.
650   Carter, T. S., Heald, C. L., Kroll, J. H., Apel, E. C., Blake, D., Coggon, M., Edtbauer, A., Gkatzelis, G., Hornbrook,
651   R. S., and Peischl, J.: An improved representation of fire non-methane organic gases (NMOGs) in models:
652   emissions to reactivity, Atmos. Chem. Phys., 22, 12093-12111, 2022.
653   Chandramouli, C. and General, R.: Census of india 2011, Provisional Population Totals. New Delhi: Government
654   of India, 409-413, 2011.
655   Chen, Y.-T., Chen, H.-W., Domanski, D., Smith, D. S., Liang, K.-H., Wu, C.-C., Chen, C.-L., Chung, T., Chen,
656   M.-C., and Chang, Y.-S.: Multiplexed quantification of 63 proteins in human urine by multiple reaction
657   monitoring-based mass spectrometry for discovery of potential bladder cancer biomarkers, Journal of
658   proteomics, 75, 3529-3545, 2012.
659   Chmaj-Wierzchowska, K., Kampioni, M., Wilczak, M., Sajdak, S., and Opala, T.: Novel markers in the
660   diagnostics of endometriomas: Urocortin, ghrelin, and leptin or leukocytes, fibrinogen, and CA-125?,
661   Taiwanese Journal of Obstetrics and Gynecology, 54, 126-130, 2015.
662   Christian, T. J.: Comprehensive laboratory measurements of biomass-burning emissions: 2. First intercomparison
663   of open-path FTIR, PTR-MS, and GC-MS/FID/ECD, J. Geophys. Res., 109, 10.1029/2003jd003874, 2004.

Christian, T. J., Kleiss, B., Yokelson, R. J., Holzinger, R., Crutzen, P., Hao, W. M., Saharjo, B., and Ward, D. E.: Comprehensive laboratory measurements of biomass-burning emissions: 1. Emissions from Indonesian, African, and other fuels, Journal of Geophysical Research: Atmospheres, 108, 2003.

Donahue, N. M., Kroll, J., Pandis, S. N., and Robinson, A. L.: A two-dimensional volatility basis set–Part 2: Diagnostics of organic-aerosol evolution, Atmos. Chem. Phys., 12, 615-634, 2012.

Donahue, N. M., Robinson, A., Stanier, C., and Pandis, S.: Coupled partitioning, dilution, and chemical aging of semivolatile organics, Environmental science & technology, 40, 2635-2643, 2006.

Font-Palma, C.: Methods for the Treatment of Cattle Manure—A Review, C, 5, 10.3390/c5020027, 2019.

Font, A., Ciupek, K., Butterfield, D., and Fuller, G.: Long-term trends in particulate matter from wood burning in the United Kingdom: Dependence on weather and social factors, Environ. Pollut., 314, 120105, 2022.

Fourtziou, L., Liakakou, E., Stavroulas, I., Theodosi, C., Zarmpas, P., Psiloglou, B., Sciare, J., Maggos, T., Bairachtari, K., and Bougiatioti, A.: Multi-tracer approach to characterize domestic wood burning in Athens (Greece) during wintertime, Atmos. Environ., 148, 89-101, 2017.

Greenberg, J., Friedli, H., Guenther, A., Hanson, D., Harley, P., and Karl, T.: Volatile organic emissions from the distillation and pyrolysis of vegetation, Atmos. Chem. Phys., 6, 81-91, 2006.

Grieshop, A., Logue, J., Donahue, N., and Robinson, A.: Laboratory investigation of photochemical oxidation of organic aerosol from wood fires 1: measurement and simulation of organic aerosol evolution, Atmos. Chem. Phys., 9, 1263-1277, 2009.

Guo, J., Wu, H., Zhao, Z., Wang, J., and Liao, H.: Review on health impacts from domestic coal burning: emphasis on endemic fluorosis in Guizhou Province, Southwest China, Reviews of Environmental Contamination and Toxicology Volume 258, 1-25, 2021.

Hatch, L. E., Rivas-Ubach, A., Jen, C. N., Lipton, M., Goldstein, A. H., and Barsanti, K. C.: Measurements of I/SVOCs in biomass-burning smoke using solid-phase extraction disks and two-dimensional gas chromatography, Atmos. Chem. Phys., 18, 17801-17817, 2018.

Hatch, L. E., Yokelson, R. J., Stockwell, C. E., Veres, P. R., Simpson, I. J., Blake, D. R., Orlando, J. J., and Barsanti, K. C.: Multi-instrument comparison and compilation of non-methane organic gas emissions from biomass burning and implications for smoke-derived secondary organic aerosol precursors, Atmos. Chem. Phys., 17, 1471-1489, 10.5194/acp-17-1471-2017, 2017.

Hatch, L. E., Jen, C. N., Kreisberg, N. M., Selimovic, V., Yokelson, R. J., Stamatis, C., York, R. A., Foster, D., Stephens, S. L., and Goldstein, A. H.: Highly speciated measurements of terpenoids emitted from laboratory and mixed-conifer forest prescribed fires, Environmental Science & Technology, 53, 9418-9428, 2019.

He, C., Murray, F., and Lyons, T.: Seasonal variations in monoterpene emissions from Eucalyptus species, Chemosphere-Global change science, 2, 65-76, 2000.

Hellén, H., Tykkä, T., and Hakola, H.: Importance of monoterpenes and isoprene in urban air in northern Europe, Atmos. Environ., 59, 59-66, 10.1016/j.atmosenv.2012.04.049, 2012.

Heringa, M. F., DeCarlo, P. F., Chirico, R., Tritscher, T., Dommen, J., Weingartner, E., Richter, R., Wehrle, G., Prévôt, A. S. H., and Baltensperger, U.: Investigations of primary and secondary particulate matter of different wood combustion appliances with a high-resolution time-of-flight aerosol mass spectrometer, Atmos. Chem. Phys., 11, 5945-5957, 10.5194/acp-11-5945-2011, 2011.

Hill Bembenic, M. A.: The chemistry of subcritical water reactions of a hardwood derived lignin and lignin model compounds with nitrogen, hydrogen, carbon monoxide and carbon dioxide, 2011.

Hodzic, A., Jimenez, J. L., Madronich, S., Canagaratna, M. R., DeCarlo, P. F., Kleinman, L., and Fast, J.: Modeling organic aerosols in a megacity: potential contribution of semi-volatile and intermediate volatility primary organic compounds to secondary organic aerosol formation, Atmos. Chem. Phys., 10, 5491-5514, 10.5194/acp-10-5491-2010, 2010.

Huang, W., Li, H., Sarnela, N., Heikkinen, L., Tham, Y. J., Mikkilä, J., Thomas, S. J., Donahue, N. M., Kulmala, M., and Bianchi, F.: Measurement report: Molecular composition and volatility of gaseous organic

compounds in a boreal forest – from volatile organic compounds to highly oxygenated organic molecules, Atmos. Chem. Phys., 21, 8961-8977, 10.5194/acp-21-8961-2021, 2021.

Isaacman-VanWertz, G. and Aumont, B.: Impact of organic molecular structure on the estimation of atmospherically relevant physicochemical parameters, Atmos. Chem. Phys., 21, 6541-6563, 10.5194/acp-21-6541-2021, 2021.

Jasperse, B., Jakobs, C., Eikelenboom, M. J., Dijkstra, C. D., Uitdehaag, B. M., Barkhof, F., Polman, C. H., and Teunissen, C. E.: N-acetylaspartic acid in cerebrospinal fluid of multiple sclerosis patients determined by gas-chromatography-mass spectrometry, Journal of neurology, 254, 631-637, 2007.

Jin, L., Permar, W., Selimovic, V., Ketcherside, D., Yokelson, R. J., Hornbrook, R. S., Apel, E. C., Ku, I.-T., Collett Jr, J. L., and Sullivan, A. P.: Constraining emissions of volatile organic compounds from western US wildfires with WE-CAN and FIREX-AQ airborne observations, Atmos. Chem. Phys., 23, 5969-5991, 2023.

Kalogridis, A.-C., Vratolis, S., Liakakou, E., Gerasopoulos, E., Mihalopoulos, N., and Eleftheriadis, K.: Assessment of wood burning versus fossil fuel contribution to wintertime black carbon and carbon monoxide concentrations in Athens, Greece, Atmos. Chem. Phys., 18, 10219-10236, 2018.

Keller, R. G., Di Marino, D., Blindert, M., and Wessling, M.: Hydrotropic solutions enable homogeneous fenton treatment of lignin, Industrial & Engineering Chemistry Research, 59, 4229-4238, 2020.

Klein, F., Pieber, S. M., Ni, H., Stefenelli, G., Bertrand, A., Kilic, D., Pospisilova, V., Temime-Roussel, B., Marchand, N., El Haddad, I., Slowik, J. G., Baltensperger, U., Cao, J., Huang, R. J., and Prevot, A. S. H.: Characterization of Gas-Phase Organics Using Proton Transfer Reaction Time-of-Flight Mass Spectrometry: Residential Coal Combustion, Environ. Sci. Technol., 52, 2612-2617, 10.1021/acs.est.7b03960, 2018.

Koss, A. R., Sekimoto, K., Gilman, J. B., Selimovic, V., Coggon, M. M., Zarzana, K. J., Yuan, B., Lerner, B. M., Brown, S. S., and Jimenez, J. L.: Non-methane organic gas emissions from biomass burning: identification, quantification, and emission factors from PTR-ToF during the FIREX 2016 laboratory experiment, Atmos. Chem. Phys., 18, 3299-3319, 2018.

Krechmer, J., Lopez-Hilfiker, F., Koss, A., Hutterli, M., Stoermer, C., Deming, B., Kimmel, J., Warneke, C., Holzinger, R., Jayne, J., Worsnop, D., Fuhrer, K., Gonin, M., and de Gouw, J.: Evaluation of a New Reagent-Ion Source and Focusing Ion-Molecule Reactor for Use in Proton-Transfer-Reaction Mass Spectrometry, Anal. Chem., 90, 12011-12018, 10.1021/acs.analchem.8b02641, 2018.

Kumar, V., Slowik, J. G., Baltensperger, U., Prevot, A. S. H., and Bell, D. M.: Time-Resolved Molecular Characterization of Secondary Organic Aerosol Formed from OH and NO(3) Radical Initiated Oxidation of a Mixture of Aromatic Precursors, Environ. Sci. Technol., 57, 11572-11582, 10.1021/acs.est.3c00225, 2023.

Li, H., Riva, M., Rantala, P., Heikkinen, L., Daellenbach, K., Krechmer, J. E., Flaud, P.-M., Worsnop, D., Kulmala, M., Villenave, E., Perraudin, E., Ehn, M., and Bianchi, F.: Terpenes and their oxidation products in the French Landes forest: insights from Vocus PTR-TOF measurements, Atmos. Chem. Phys., 20, 1941-1959, 10.5194/acp-20-1941-2020, 2020.

Li, K., Zhang, J., Bell, D. M., Wang, T., Lamkaddam, H., Cui, T., Qi, L., Surdu, M., Wang, D., Du, L., Haddad, I. E., Slowik, J. G., and Prevot, A. S. H.: Uncovering the dominant contribution of intermediate volatility compounds in secondary organic aerosol formation from biomass-burning emissions, National Science Review, 10.1093/nsr/nwae014, 2024.

Li, X., Wang, S., Duan, L., Hao, J., Li, C., Chen, Y., and Yang, L.: Particulate and Trace Gas Emissions from Open Burning of Wheat Straw and Corn Stover in China, Environ. Sci. Technol., 41, 6052-6058, 10.1021/es0705137, 2007.

Li, Y., Pöschl, U., and Shiraiwa, M.: Molecular corridors and parameterizations of volatility in the chemical evolution of organic aerosols, Atmos. Chem. Phys., 16, 3327-3344, 10.5194/acp-16-3327-2016, 2016.

Li, Z., Wang, S., Li, S., Wang, X., Huang, G., Chang, X., Huang, L., Liang, C., Zhu, Y., and Zheng, H.: High-resolution emission inventory of full-volatility organic compounds from cooking in China during 2015–2021, Earth System Science Data, 15, 5017-5037, 2023.

Liu, C., Zhang, C., Mu, Y., Liu, J., and Zhang, Y.: Emission of volatile organic compounds from domestic coal stove with the actual alternation of flaming and smoldering combustion processes, Environ. Pollut., 221, 385-391, 10.1016/j.envpol.2016.11.089, 2017.

Liu, Y., Shao, M., Fu, L., Lu, S., Zeng, L., and Tang, D.: Source profiles of volatile organic compounds (VOCs) measured in China: Part I, Atmos. Environ., 42, 6247-6260, 10.1016/j.atmosenv.2008.01.070, 2008.

Liu, Y., Liao, B., Guo, W., Fu, Y., Sun, W., Fu, Y., Wang, D., and Kang, H.: Study on Separation and Purification of Chemical Components of Dichloromethane from Pine Needle Extract, IOP Conference Series: Earth and Environmental Science, 714, 032039, 2021.

Loebel Roson, M., Duruisseau-Kuntz, R., Wang, M., Klimchuk, K., Abel, R. J., Harynuk, J. J., and Zhao, R.: Chemical Characterization of Emissions Arising from Solid Fuel Combustion—Contrasting Wood and Cow Dung Burning, ACS Earth and Space Chemistry, 5, 2925-2937, 10.1021/acsearthspacechem.1c00268, 2021.

Ma, Y. and Hays, M. D.: Thermal extraction–two-dimensional gas chromatography–mass spectrometry with heart-cutting for nitrogen heterocyclics in biomass burning aerosols, J. Chromatogr. A, 1200, 228-234, 2008.

Majluf, F. Y., Krechmer, J. E., Daube, C., Knighton, W. B., Dyroff, C., Lambe, A. T., Fortner, E. C., Yacovitch, T. I., Roscioli, J. R., Herndon, S. C., Worsnop, D. R., and Canagaratna, M. R.: Mobile Near-Field Measurements of Biomass Burning Volatile Organic Compounds: Emission Ratios and Factor Analysis, Environmental Science & Technology Letters, 9, 383-390, 10.1021/acs.estlett.2c00194, 2022.

Mann, H. B. and Whitney, D. R.: On a test of whether one of two random variables is stochastically larger than the other, Annals of Mathematical Statistics, 18, 50-60, 10.1214/aoms/1177730491, 1947.

Mastral, A. M. and Callen, M. S.: A review on polycyclic aromatic hydrocarbon (PAH) emissions from energy generation, Environmental Science & Technology, 34, 3051-3057, 2000.

Nagai, K., Uranbileg, B., Chen, Z., Fujioka, A., Yamazaki, T., Matsumoto, Y., Tsukamoto, H., Ikeda, H., Yatomi, Y., and Chiba, H.: Identification of novel biomarkers of hepatocellular carcinoma by high-definition mass spectrometry: Ultrahigh-performance liquid chromatography quadrupole time-of-flight mass spectrometry and desorption electrospray ionization mass spectrometry imaging, Rapid Commun. Mass Spectrom., 34, e8551, 2020.

Nelson, R. M.: An evaluation of the carbon balance technique for estimating emission factors and fuel consumption in forest fires, US Department of Agriculture, Forest Service, Southeastern Forest Experiment …1982.

Ni, H., Huang, R.-J., Pieber, S. M., Corbin, J. C., Stefenelli, G., Pospisilova, V., Klein, F., Gysel-Beer, M., Yang, L., and Baltensperger, U.: Brown carbon in primary and aged coal combustion emission, Environmental Science & Technology, 55, 5701-5710, 2021.

Noe, S. M., Hüve, K., Niinemets, Ü., and Copolovici, L.: Seasonal variation in vertical volatile compounds air concentrations within a remote hemiboreal mixed forest, Atmos. Chem. Phys., 12, 3909-3926, 10.5194/acp-12-3909-2012, 2012.

Nomura, F., Tomonaga, T., Sogawa, K., Ohashi, T., Nezu, M., Sunaga, M., Kondo, N., Iyo, M., Shimada, H., and Ochiai, T.: Identification of novel and downregulated biomarkers for alcoholism by surface enhanced laser desorption/ionization-mass spectrometry, Proteomics, 4, 1187-1194, 2004.

Oberschelp, C., Pfister, S., Raptis, C., and Hellweg, S.: Global emission hotspots of coal power generation, Nature Sustainability, 2, 113-121, 2019.

Permar, W., Wang, Q., Selimovic, V., Wielgasz, C., Yokelson, R. J., Hornbrook, R. S., Hills, A. J., Apel, E. C., Ku, I. T., and Zhou, Y.: Emissions of trace organic gases from Western US wildfires based on WE-CAN aircraft measurements, J. Geophys. Res. Atmos., 126, e2020JD033838, 2021.

Ren, Q. and Zhao, C.: Evolution of fuel-N in gas phase during biomass pyrolysis, Renewable and Sustainable Energy Reviews, 50, 408-418, 2015.

Riva, M., Rantala, P., Krechmer, J. E., Peräkylä, O., Zhang, Y., Heikkinen, L., Garmash, O., Yan, C., Kulmala, M., Worsnop, D., and Ehn, M.: Evaluating the performance of five different chemical ionization techniques

805   for detecting gaseous oxygenated organic species, Atmospheric Measurement Techniques, 12, 2403-2421,
806   10.5194/amt-12-2403-2019, 2019.

807 Robinson, A. L., Donahue, N. M., Shrivastava, M. K., Weitkamp, E. A., Sage, A. M., Grieshop, A. P., Lane, T.
808   E., Pierce, J. R., and Pandis, S. N.: Rethinking organic aerosols: Semivolatile emissions and photochemical
809   aging, Sci, 315, 1259-1262, 2007.

810 Sarangi, B., Aggarwal, S. G., and Gupta, P. K.: Performance check of particle size standards within and after
811   shelf-life using differential mobility analyzer, Journal of Aerosol Science, 103, 24-37, 2017.

812 Sarkar, C., Sinha, V., Kumar, V., Rupakheti, M., Panday, A., Mahata, K. S., Rupakheti, D., Kathayat, B., and
813   Lawrence, M. G.: Overview of VOC emissions and chemistry from PTR-TOF-MS measurements during the
814   SusKat-ABC campaign: high acetaldehyde, isoprene and isocyanic acid in wintertime air of the Kathmandu
815   Valley, Atmos. Chem. Phys., 16, 3979-4003, 10.5194/acp-16-3979-2016, 2016.

816 Schervish, M. and Donahue, N. M.: Peroxy radical chemistry and the volatility basis set, Atmos. Chem. Phys., 20,
817   1183-1199, 2020.

818 Schneider, J., Weimer, S., Drewnick, F., Borrmann, S., Helas, G., Gwaze, P., Schmid, O., Andreae, M., and
819   Kirchner, U.: Mass spectrometric analysis and aerodynamic properties of various types of combustion-related
820   aerosol particles, Int. J. Mass spectrom., 258, 37-49, 2006.

821 Sengpiel, R., Di Marino, D., Blindert, M., and Wessling, M.: 7 Hydrotropic solutions for Fenton depolymerization
822   of lignin, Extraction and Electrochemical Valorization of Lignin in Novel Electrolytes, 107, 2019.

823 Simoneit, B. R., Rogge, W., Mazurek, M., Standley, L., Hildemann, L., and Cass, G.: Lignin pyrolysis products,
824   lignans, and resin acids as specific tracers of plant classes in emissions from biomass combustion,
825   Environmental science & technology, 27, 2533-2541, 1993.

826 Stala-Szlugaj, K.: The demand for hard coal for households in Poland and the anti-smog bill, Archives of Mining
827   Sciences, 63, 701-711, 2018.

828 Stewart, G. J., Acton, W. J. F., Nelson, B. S., Vaughan, A. R., Hopkins, J. R., Arya, R., Mondal, A., Jangirh, R.,
829   Ahlawat, S., Yadav, L., Sharma, S. K., Dunmore, R. E., Yunus, S. S. M., Hewitt, C. N., Nemitz, E., Mullinger,
830   N., Gadi, R., Sahu, L. K., Tripathi, N., Rickard, A. R., Lee, J. D., Mandal, T. K., and Hamilton, J. F.:
831   Emissions of non-methane volatile organic compounds from combustion of domestic fuels in Delhi, India,
832   Atmos. Chem. Phys., 21, 2383-2406, 10.5194/acp-21-2383-2021, 2021a.

833 Stewart, G. J., Nelson, B. S., Acton, W. J. F., Vaughan, A. R., Farren, N. J., Hopkins, J. R., Ward, M. W., Swift,
834   S. J., Arya, R., Mondal, A., Jangirh, R., Ahlawat, S., Yadav, L., Sharma, S. K., Yunus, S. S. M., Hewitt, C.
835   N., Nemitz, E., Mullinger, N., Gadi, R., Sahu, L. K., Tripathi, N., Rickard, A. R., Lee, J. D., Mandal, T. K.,
836   and Hamilton, J. F.: Emissions of intermediate-volatility and semi-volatile organic compounds from
837   domestic fuels used in Delhi, India, Atmos. Chem. Phys., 21, 2407-2426, 10.5194/acp-21-2407-2021, 2021b.

838 Stockwell, C. E., Veres, P. R., Williams, J., and Yokelson, R. J.: Characterization of biomass burning emissions
839   from cooking fires, peat, crop residue, and other fuels with high-resolution proton-transfer-reaction time-of-
840   flight mass spectrometry, Atmos. Chem. Phys., 15, 845-865, 10.5194/acp-15-845-2015, 2015.

841 Sun, Y., Chen, Y., Sun, C., Liu, H., Wang, Y., and Jiang, X.: Analysis of volatile organic compounds from patients
842   and cell lines for the validation of lung cancer biomarkers by proton-transfer-reaction mass spectrometry,
843   Analytical Methods, 11, 3188-3197, 2019.

844 Tao, S., Ru, M., Du, W., Zhu, X., Zhong, Q., Li, B., Shen, G., Pan, X., Meng, W., and Chen, Y.: Quantifying the
845   rural residential energy transition in China from 1992 to 2012 through a representative national survey,
846   Nature Energy, 3, 567-573, 2018.

847 Teunissen, C., Koel-Simmelink, M., Pham, T., Knol, J., Khalil, M., Trentini, A., Killestein, J., Nielsen, J., Vrenken,
848   H., and Popescu, V.: Identification of biomarkers for diagnosis and progression of MS by MALDI-TOF mass
849   spectrometry, Multiple Sclerosis Journal, 17, 838-850, 2011.

850 Tkacik, D. S., Robinson, E. S., Ahern, A., Saleh, R., Stockwell, C., Veres, P., Simpson, I. J., Meinardi, S., Blake,
851   D. R., Yokelson, R. J., Presto, A. A., Sullivan, R. C., Donahue, N. M., and Robinson, A. L.: A dual-chamber
852   method for quantifying the effects of atmospheric perturbations on secondary organic aerosol formation from

biomass burning emissions, Journal of Geophysical Research: Atmospheres, 122, 6043-6058, 10.1002/2016jd025784, 2017.

Tong, Y., Pospisilova, V., Qi, L., Duan, J., Gu, Y., Kumar, V., Rai, P., Stefenelli, G., Wang, L., Wang, Y., Zhong, H., Baltensperger, U., Cao, J., Huang, R.-J., Prévôt, A. S. H., and Slowik, J. G.: Quantification of solid fuel combustion and aqueous chemistry contributions to secondary organic aerosol during wintertime haze events in Beijing, Atmos. Chem. Phys., 21, 9859-9886, 10.5194/acp-21-9859-2021, 2021.

Tritten, L., Keiser, J., Godejohann, M., Utzinger, J., Vargas, M., Beckonert, O., Holmes, E., and Saric, J.: Metabolic profiling framework for discovery of candidate diagnostic markers of malaria, Scientific reports, 3, 2769, 2013.

Wang, D. S., Lee, C. P., Krechmer, J. E., Majluf, F., Tong, Y., Canagaratna, M. R., Schmale, J., Prévôt, A. S. H., Baltensperger, U., Dommen, J., El Haddad, I., Slowik, J. G., and Bell, D. M.: Constraining the response factors of an extractive electrospray ionization mass spectrometer for near-molecular aerosol speciation, Atmospheric Measurement Techniques, 14, 6955-6972, 10.5194/amt-14-6955-2021, 2021.

Wang, T., Li, K., Bell, D. M., Zhang, J., Cui, T., Surdu, M., Baltensperger, U., Slowik, J. G., Lamkaddam, H., and El Haddad, I.: Large contribution of in-cloud production of secondary organic aerosol from biomass burning emissions, npj Climate and Atmospheric Science, 7, 149, 2024.

Warneke, C., Roberts, J. M., Veres, P., Gilman, J., Kuster, W. C., Burling, I., Yokelson, R., and de Gouw, J. A.: VOC identification and inter-comparison from laboratory biomass burning using PTR-MS and PIT-MS, Int. J. Mass spectrom., 303, 6-14, 10.1016/j.ijms.2010.12.002, 2011.

Weber, K. T. and Yadav, R.: Spatiotemporal trends in wildfires across the Western United States (1950–2019), Remote Sensing, 12, 2959, 2020.

Weimer, S., Alfarra, M. R., Schreiber, D., Mohr, M., Prévôt, A. S. H., and Baltensperger, U.: Organic aerosol mass spectral signatures from wood-burning emissions: Influence of burning conditions and wood type, J. Geophys. Res., 113, 10.1029/2007jd009309, 2008.

White, R., Pulford, E., Elliot, D. J., Thurgood, L. A., and Klebe, S.: Quantitative mass spectrometry to identify protein markers for diagnosis of malignant pleural mesothelioma, Journal of proteomics, 192, 374-382, 2019.

Wiedensohler, A., Wiesner, A., Weinhold, K., Birmili, W., Hermann, M., Merkel, M., Müller, T., Pfeifer, S., Schmidt, A., and Tuch, T.: Mobility particle size spectrometers: Calibration procedures and measurement uncertainties, Aerosol Sci. Technol., 52, 146-164, 2018.

Wilcoxon, F.: Individual Comparisons by Ranking Methods, Biometrics Bulletin, 1, 80-83, 10.2307/3001968, 1945.

Williams, A. P., Allen, C. D., Macalady, A. K., Griffin, D., Woodhouse, C., Meko, D. M., Swetnam, T. W., Rauscher, S. A., Seager, R., and Grissino-Mayer, H. D.: Temperature as a potent driver of regional forest drought stress and tree mortality, 2012.

Wu, D., Zheng, H., Li, Q., Jin, L., Lyu, R., Ding, X., Huo, Y., Zhao, B., Jiang, J., and Chen, J.: Toxic potency-adjusted control of air pollution for solid fuel combustion, Nature Energy, 7, 194-202, 2022.

Yuan, B., Koss, A. R., Warneke, C., Coggon, M., Sekimoto, K., and de Gouw, J. A.: Proton-Transfer-Reaction Mass Spectrometry: Applications in Atmospheric Sciences, Chem Rev, 117, 13187-13229, 10.1021/acs.chemrev.7b00325, 2017.

Zhang, J. and Smith, K. R.: Household air pollution from coal and biomass fuels in China: measurements, health impacts, and interventions, Environ. Health Perspect., 115, 848-855, 2007.

Zhang, J., Li, K., Wang, T., Gammelsæter, E., Cheung, R. K., Surdu, M., Bogler, S., Bhattu, D., Wang, D. S., and Cui, T.: Bulk and molecular-level composition of primary organic aerosol from wood, straw, cow dung, and plastic burning, Atmos. Chem. Phys., 23, 14561-14576, 2023.

Zhang, J., Smith, K., Ma, Y., Ye, S., Jiang, F., Qi, W., Liu, P., Khalil, M., Rasmussen, R., and Thorneloe, S.: Greenhouse gases and other airborne pollutants from household stoves in China: a database for emission factors, Atmos. Environ., 34, 4537-4549, 2000.

Zhang, X., Xu, J., Zhai, L., and Zhao, W.: Characterization of Aerosol Properties from the Burning Emissions of Typical Residential Fuels on the Tibetan Plateau, Environ. Sci. Technol., 56, 14296-14305, 10.1021/acs.est.2c04211, 2022.

Zhao, B., Wang, S., Donahue, N. M., Jathar, S. H., Huang, X., Wu, W., Hao, J., and Robinson, A. L.: Quantifying the effect of organic aerosol aging and intermediate-volatility emissions on regional-scale aerosol pollution in China, Scientific reports, 6, 28815, 2016.

Zhao, N., Li, B., Ahmad, R., Ding, F., Zhou, Y., Li, G., Zayan, A. M. I., and Dong, R.: Dynamic relationships between real-time fuel moisture content and combustion-emission-performance characteristics of wood pellets in a top-lit updraft cookstove, Case Studies in Thermal Engineering, 28, 10.1016/j.csite.2021.101484, 2021.